Sorting Nexin 27 regulates basal and activity-dependent trafficking of AMPARs

Natasha K. Hussain[a,b], Graham H. Diering[a,b], Jonathan Sole[a,b], Victor Anggono[c], and Richard L. Huganir[a,b,1]

[a]Solomon H. Snyder Department of Neuroscience, [b]Howard Hughes Medical Institute, Johns Hopkins University School of Medicine, Baltimore, MD 21205; and [c]Clem Jones Centre for Ageing Dementia Research, Queensland Brain Institute, The University of Queensland, Brisbane 4072, Queensland, Australia

Contributed by Richard L. Huganir, July 3, 2014 (sent for review April 4, 2014)

Activity-dependent changes in synaptic strength have long been postulated as cellular correlates of learning and memory. Long-term potentiation (LTP), a well characterized form of synaptic plasticity, is often expressed as an increase in the number of postsynaptic AMPA-type glutamate receptors (AMPARs). Although the precise molecular mechanisms governing LTP remain elusive, this study identifies one member of the sorting nexin family, Sorting Nexin 27 (SNX27), as a critical component in this process. The ability of sorting nexins to bind specific phospholipids as well as their propensity to form protein–protein complexes, points to a role for these proteins in membrane trafficking and protein sorting. Here, we demonstrate that SNX27 binds to AMPARs, and that this interaction is regulated in an activity-dependent manner. Furthermore, we provide evidence that SNX27 is synaptically enriched and its level of expression regulates targeting of AMPARs to the neuronal surface. Loss of SNX27 abolishes recruitment of surface AMPARs during chemical LTP. Collectively, our data suggest a role for SNX27 in modulating synaptic plasticity through regulated interaction with AMPARs.

PX domain | postsynaptic density | proteomics | PDZ-domain

Modulation of α-amino-3-hydroxy-5-methyl-4-isoxazolepropionic acid receptor (AMPAR) activity, whether through changes in surface expression or conductance, contributes significantly to the dynamic nature of neuronal networks. During long-term potentiation (LTP), AMPARs are delivered to the plasma membrane to induce an early burst and for long-term maintenance of synaptic potentiation (1). Importantly, aberrant AMPAR trafficking has been found to contribute to impaired synaptic plasticity and deficits in learning and memory (2–4) for review see (5). AMPAR trafficking, which contributes to changes in synaptic strength, is facilitated through a complex and fluidic endosomal recycling network (6, 7). Beneath the plasma membrane, the endosomal network comprises a series of interconnected membranous compartments responsible for recycling proteins. Internalized receptors enter the early endosome to be sorted for lysosomal and proteasomal degradation, or are recycled back to the plasma membrane (6, 7). Although a great deal is known about the mechanisms for protein sorting along the degradative pathway, a comprehensive delineation of how cargo is selectively reinserted into the neuronal surface remains to be determined. Studies have shown that protein complexes can regulate AMPAR trafficking from early endosomes back to the plasma membrane (8–10). Recycling of AMPAR-containing endosomes to the plasma membrane is critical for AMPAR localization, particularly after LTP induction; knockdown or mutation of proteins associated with the recycling machinery redistributes AMPARs from the spine surface to internal endosomes (8–10). Thus, recycling endosomes and their trafficking may provide a mechanistic link between synaptic potentiation and AMPAR insertion.

Further insight into the mechanisms of sorting at the level of endosomes comes from the characterization of protein–protein interactions. Several proteins have been identified that can promote or destabilize AMPA receptor surface expression/targeting through direct interaction with AMPARs (1, 6, 7). Much focus has been directed at identifying molecules that specifically interact with the C-terminal domains of AMPAR subunits as they are accessible to the intracellular milieu of the cell. Using this approach here we identified sorting nexin 27 (SNX27) as an AMPAR binding partner.

SNX27 is a member of the sorting nexin family of proteins. Sorting nexins (SNXs) are a diverse group of cytoplasmic and membrane-associated proteins implicated in endocytosis and protein trafficking. They have been identified across phyla, from yeast to mammals, and their essential role in many endosomal recycling pathways is evolutionarily conserved (11). The hallmark of the sorting nexin family is the presence of a phox-homology domain (PX), a 100- to 140-aa sequence shown to interact with phosphatidylinositol phosphate (PIP) of structural membrane lipids (12). This protein–lipid interaction serves as a mechanism by which sorting nexin proteins can dock at the plasma membrane or endosomes, as these membranes are enriched in various PIPs (11).

Outside of their PX domain, SNXs are a structurally diverse group of proteins. Several members contain other important functional domains, including those capable of mediating protein–protein interaction. Current literature suggests duality to SNXs function in endosomal trafficking: They use their membrane association domains to localize to endosomes while using their protein–protein interaction domains to promote protein complex formation (11). Thus, SNXs act as critical adaptor molecules; orchestrating protein recycling through recognition and concentration of specific cargo, driving membrane remodeling and eliciting scission to form a cargo-enriched carrier (11, 13).

SNX27 is of particular interest for synaptic protein recycling, as it is the only sorting nexin to contain a postsynaptic density 95/discs large/zona occludens (PDZ) domain, and is implicated in mediating PDZ-directed sorting from endosomes to the plasma

Significance

AMPA-type glutamate receptors (AMPARs) are principal regulators of synaptic signaling in the brain. Modulation of AMPA receptor activity, whether through changes in surface expression or conductance, contributes significantly to the dynamic nature of neuronal networks. AMPA receptor mediated-synaptic plasticity is thought to underlie learning and memory, as aberrant AMPAR trafficking contributes to impaired plasticity and to memory deficits. We demonstrate that the membrane trafficking and sorting protein, SNX27, regulates basal and activity dependent targeting of AMPA receptors to the neuronal surface. Elucidating the mechanism of receptor sorting mediated by SNX27 will not only further our understanding AMPAR-mediated changes in synaptic plasticity, but may ultimately shed light on the molecular mechanisms that govern learning.

Author contributions: N.K.H., G.H.D., V.A., and R.L.H. designed research; N.K.H., G.H.D., J.S., and V.A. performed research; N.K.H. and G.H.D. analyzed data; N.K.H., G.H.D., J.S., and R.L.H. wrote the paper.

The authors declare no conflict of interest.

[1]To whom correspondence should be addressed. Email: rhuganir@jhmi.edu.

This article contains supporting information online at www.pnas.org/lookup/suppl/doi:10.1073/pnas.1412415111/-/DCSupplemental.

membrane (14–18). The PDZ domain is a protein interaction module recognizing short amino acid motifs found at the C termini of several synaptic targets. Importantly, the PDZ ligand sequence is found on AMPAR intracellular domains, and are heavily involved mediating the assembly of multiprotein complexes, and expression of surface AMPARs (19, 20). We demonstrate that SNX27 is enriched at synapses, and that SNX27 protein level critically regulates surface AMPAR expression. We determined that the PX as well as the PDZ domain is indispensable for SNX27-mediated regulation of AMPAR surface targeting. Moreover, the interaction between SNX27 and AMPARs is regulated by neuronal activity, and SNX27 is required for chemical LTP-elicited surface AMPAR expression. Together, these findings offer a SNX-mediated mechanism for AMPAR sorting and recruitment to the plasma membrane during LTP.

Results

SNX27 Interacts with AMPARs. To identify GluA2-interacting proteins we performed pull-down assays from rat brain lysates using a GST-GluA2 C terminus fusion protein immobilized on glutathione Sepharose beads. Proteins bound to the GluA2 C terminus were eluted and resolved by SDS/PAGE and visualized using Coomassie blue staining (Fig. 1*A*). Several bands specifically eluted in the GST-GluA2 fusion protein sample visibly absent from the GST control (Fig. 1*A*, indicated with asterisks) were excised and subjected to in-gel trypsin digestion. Resulting peptides were analyzed by reverse phase liquid chromatography directly coupled to tandem mass spectrometry (LC-MS/MS). This analysis revealed eight matching peptides with 16% sequence coverage corresponding to SNX27 (Table S1). To verify these results, we performed immunoprecipitation assays from total rat brain lysates and confirmed the SXN27 and GluA2 interaction in vivo (Fig. 1*B*).

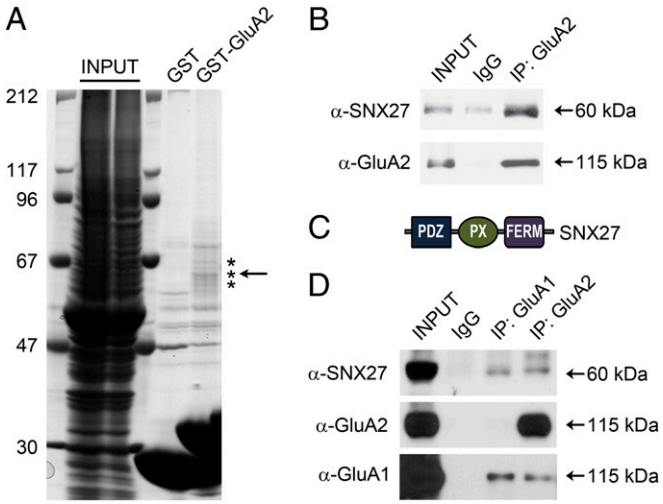

Fig. 1. Identification of SNX27 as an AMPA receptor binding protein. (*A*) GST alone or GST fused to the C-terminal domain of GluA2 was precoupled to glutathione-Sepharose and incubated with soluble rat brain lysates. Proteins bound to the beads were resolved by SDS/PAGE along with an aliquot of the soluble starting material (*INPUT*) and detected by colloidal Coomassie blue staining. The asterisk (*) indicates the position affinity-selected proteins that do not bind to GST proteins. The arrow indicates an ∼60-kDa protein band isolated for further LC-MS/MS analysis. (*B*) Immunoprecipitation from solubilized total rat brain fractions performed using control IgG or an antibody against GluA2. Brain extract proteins (INPUT), and precipitated proteins were detected by Western blot with antibodies against SNX27 or GluA2, as indicated at left. (*C*) Modular domain structure of SNX27 (FERM, band4.1/ezrin/radixin/moesin; PDZ, a postsynaptic density 95/discs large/zona occludens; PX, phox-homology). (*D*) Verification of SNX27 complex formation with GluA1 and GluA2 in cultured cortical neurons. Immunoprecipitation from extract was performed using control IgG or an antibody against GluA1 or GluA2. Precipitated proteins were detected by Western blot, along with an aliquot of the crude cell lysate (INPUT) using antibodies against SNX27 or GluA2, and GluA1. Molecular weight of proteins is indicated in kilodaltons (kDa) at right.

Because SNX27 contains a PX domain, it is typified as a member of the sorting nexin family, proteins implicated in membrane-protein trafficking (11). However, SNX27 is unique among sorting nexins in that it is the only member that includes a PDZ domain (Fig. 1*C*). The PDZ domain of SNX27 interacts with numerous C-terminal PDZ-ligand containing proteins, including Kir3 channels, β -Pix, VPS26, as well as *N*-Methyl-D-aspartate (NMDA) 2C, β-adrenergic, and 5-hydroxytrptamine type 4(a) [5-HT4(a)] receptors (14–16, 18, 21–26). Given our finding that GluA2 binds SNX27, coupled with the fact that GluA1 contains a PDZ-ligand at its C terminus, we reasoned that SNX27 may also interact with GluA1. Immunoprecipitation of AMPA receptors from cultured cortical neuron cell lysate demonstrate that SNX27 can form a complex with GluA1 as well as GluA2 in vivo (Fig. 1*D*).

SNX27 Is an Endosomal Protein that Is Also Enriched in Postsynaptic Densities. We examined the cellular localization of overexpressed SNX27 in hippocampal neurons, as antibodies for endogenous SNX27 were ineffective for immunocytochemistry. Dissociated hippocampal neurons were grown for 18 d in vitro followed by 1 d after GFP-SNX27 transfection. GFP-SNX27 expressed as punctae distributed throughout the cell body and within neuronal processes. These punctae partially colocalized with both an endosomal (early endosomal marker1, EEA1) and synaptic marker (PSD95) (Fig. 2*A*). Consistent with a putative role in glutamatergic receptor regulation, GFP-SNX27 partially overlapped with (arrows) or was in close apposition to (arrowheads) endogenous GluN1, surface GluA1 (sGluA1), as well as surface GluA2 (sGluA2) expressed along dendrites and in spines (Fig. 2*A*).

Our identification of SNX27 targeting to PSD95 in hippocampal cultures suggests that SNX27 should exist within the postsynaptic density (PSD). We analyzed the distribution of endogenous SNX27 in a subcellular fractionation of cultured cortical neuron homogenates leading to purified PSDs. We determined that SNX27 is not only expressed within synapses, it is a specifically enriched component of the PSD, similar to GluA1 and PSD-95 (Fig. 2*B*). Collectively, our data demonstrate that SNX27 is an AMPAR-binding protein found not only in endosomal compartments, but also concentrated at synapses.

PX and PDZ Domains of SNX27 Are Critical Regulators of Surface AMPAR Expression. SNX27 modulates recycling of several protein receptors (14–16, 21). To assess whether SNX27 similarly regulates surface expression of AMPARs we transfected wildtype (GFP-SNX27), a deletion construct defective in lipid binding (GFP-SNX27ΔPX), or a point mutant disrupting PDZ ligand association (GFP-SNX27H112A) form of SNX27 in hippocampal neurons (Fig. 3 *A* and *B* and Fig. S1). Quantification of the integrated intensity for sGluA1 and sGluA2 dendritic clusters each revealed a robust increase following two days of wild-type SNX27 overexpression (Fig. 3 *C* and *D*, respectively). In contrast, expression of GFP-SNX27ΔPX or GFP-SNX27H112A failed to alter surface AMPA receptor expression relative to control (Fig. 3 *C* and *D*). Thus, appropriate PX domain-mediated targeting to membrane, and specific PDZ-domain mediated interactions are required for SNX27 to exert functional control over surface AMPARs trafficking.

Given the robust effect of enhanced SNX27 expression on surface AMPAR content, we asked whether loss of SNX27 also modulates GluA1 and GluA2 function. To begin, we knocked down expression of SNX27 using plasmid-based short hairpin RNA (shRNA) interference in cortical neurons (Fig. S2*A*), and were able to significantly reduce neuronal SNX27 expression compared with control (Fig. S2*B*) (16). Vector control or SNX27

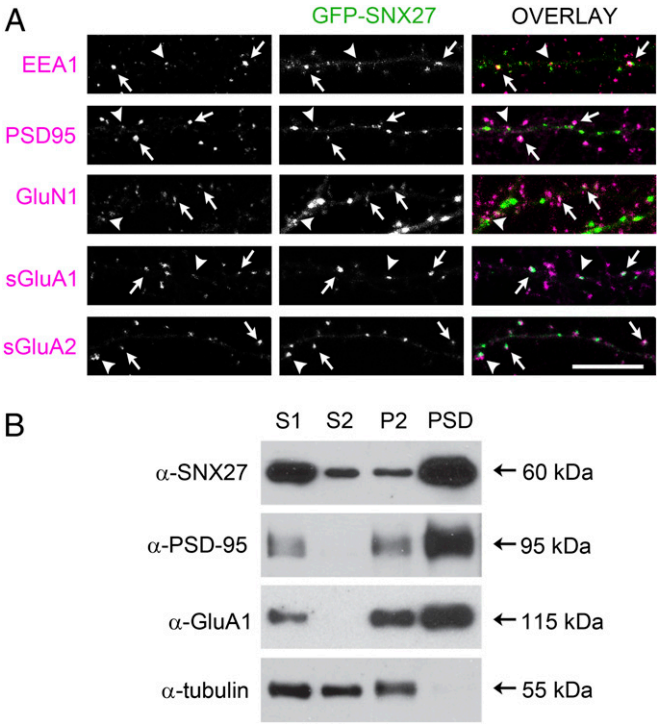

Fig. 2. Subcellular distribution of SNX27 in neurons. (*A*) Confocal microscopy of 18–20 d old hippocampal neurons stained (indicated at left) one day after transfection with GFP-tagged SNX27. Arrows indicate overlap, arrowheads indicate closely apposed punctae of neuronal marker with inherent fluorescence from GFP-SNX27 punctae. (Scale bars, 10 μm.) (*B*) SNX27 is enriched in PSD. Western blot analyses of 18-d-old cortical neuron subcellular fractionation for crude postnuclear fraction (S1), cytosolic proteins (S2), membrane fraction (P2), and Trition X-100–extracted PSD (1 μg of protein for each fraction). Antibodies for immunoblotting are indicated at left; molecular weight of proteins is indicated in kilodaltons (kDa) at right.

shRNA transfected neurons were treated by cell-surface biotinylation and surface and total proteins examined by Western blot. SNX27 depletion significantly decreased surface and total levels of GluA1, GluA2, and GluA3:00 AMPA receptor subunits, as well as GluN1, the obligatory NMDA receptor subunit (Fig. 4 *A*–*C*). Surface and total levels of Na^+/H^+ exchanger 1 (NHE1), a resident plasma membrane protein (27), were not affected by loss of SNX27 (Fig. 4 *A*–*C*) demonstrating the specificity of our results.

To corroborate these biochemical findings we examined the functional consequence of SNX27 knockdown on AMPARs in hippocampal cultures (Fig. 4 *D* and *E*). The integrated intensity of dendritic GluA1 (Fig. 4*F*) and GluA2 (Fig. 4*G*) surface clusters was dramatically decreased following SNX27 protein down-regulation. Importantly, the observed defect in AMPA receptor trafficking is specific to SNX27 loss, as coexpression of an shRNA resistant SNX27 cDNA completely restored surface trafficking of GluA1 and GluA2 to control levels (Fig. 4 *D*–*G*). These data demonstrate that intact expression and targeting of SNX27 is crucial for normal surface expression of glutamatergic receptors.

Activity-Dependent Enhancement of Surface AMPAR Requires SNX27 Expression. Rapid AMPA receptor trafficking to the dendritic membrane surface is a salient feature of enhanced transmission during LTP in the hippocampus (28–33) and for review, see ref. 34. Given our demonstration that SNX27 regulates surface AMPAR expression, we posit that synaptic activity may also impact AMPAR-mediated interaction with SNX27. Bath application of glycine onto hippocampal neurons activates synaptic NMDARs in response to spontaneously released glutamate in dissociated hippocampal neurons, and causes rapid membrane insertion of AMPARs (30, 35, 36). We used this chemical stimulation protocol mimicking LTP (cLTP) to characterize AMPAR-mediated protein interactions following enhanced neuronal activity. Consistent with our previous results, immunoprecipitation of GluA1 from a total extract isolated from unstimulated cortical neurons efficiently coimmunoprecipitated SNX27 (Fig. 5 *A* and *B*). However, 5 min of glycine stimulation followed by 10 min recovery in artificial cerebrospinal fluid (ACSF) lead to increased binding of GluA1 and SNX27. Twenty minutes following induction of cLTP this interaction was significantly enhanced (Fig. 5 *A* and *B*).

Next we used cell-surface biotinylation and Western blot to examine the role of SNX27 in regulated AMPAR surface targeting during cLTP. As shown previously, NMDA receptor activation by glycine resulted in a significant increase in sGluA1 levels in a time-dependent manner (Fig. 5 *C* and *D*). Notably, sGluA1 levels were significantly increased 20 min following

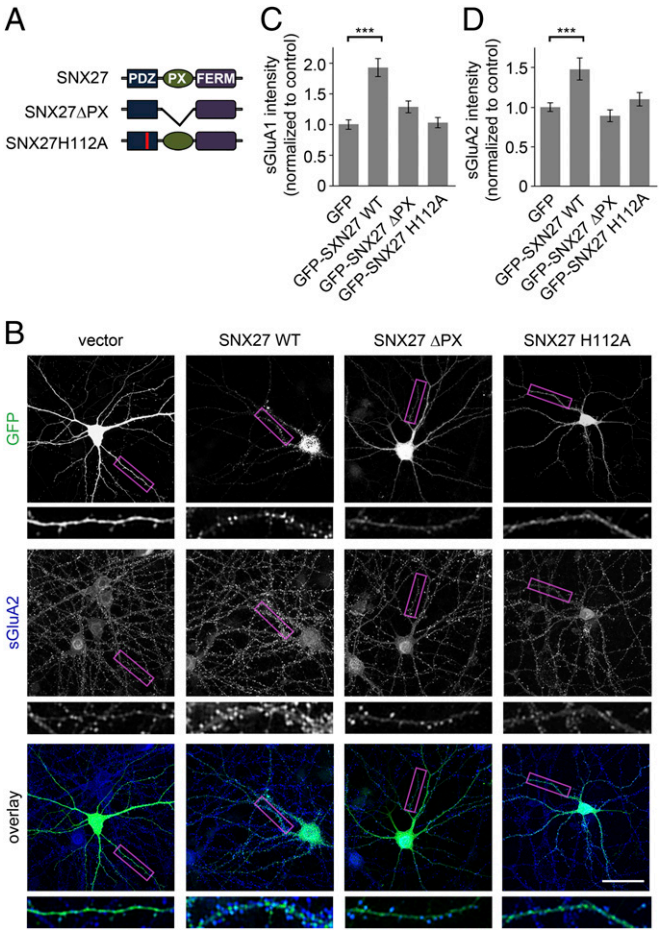

Fig. 3. SNX27 PX and PDZ domains are required for SNX27-mediated modulation of AMPARs. (*A*) Schematic diagram of wild-type SNX27 (WT), SNX27 PX domain deletion (SNX27 ΔPX), or SNX27 harboring a point mutation within the PDZ domain (SNX27 H112A) constructs used for overexpression in neurons. (*B*) Representative images of 18- to 20-d-old hippocampal neurons transfected for 24 h with GFP or GFP-tagged SNX27 constructs as indicated at top, and immunostained for sGluA2 expression. (Scale bars, 40 μm.) Enlarged dendritic regions are 40-μm segments. (*C* and *D*) Wild-type SNX27 expression increases surface AMPAR expression. Bar graph of mean integrated intensity of dendritic sGluA1 (*C*) and sGluA2 (*D*) clusters normalized to GFP vector-transfected hippocampal neurons. Error bars indicate ± SEM ***$P < 0.0001$, relative to empty vector-transfected neurons, ANOVA. $n \geq 12$ neurons for each.

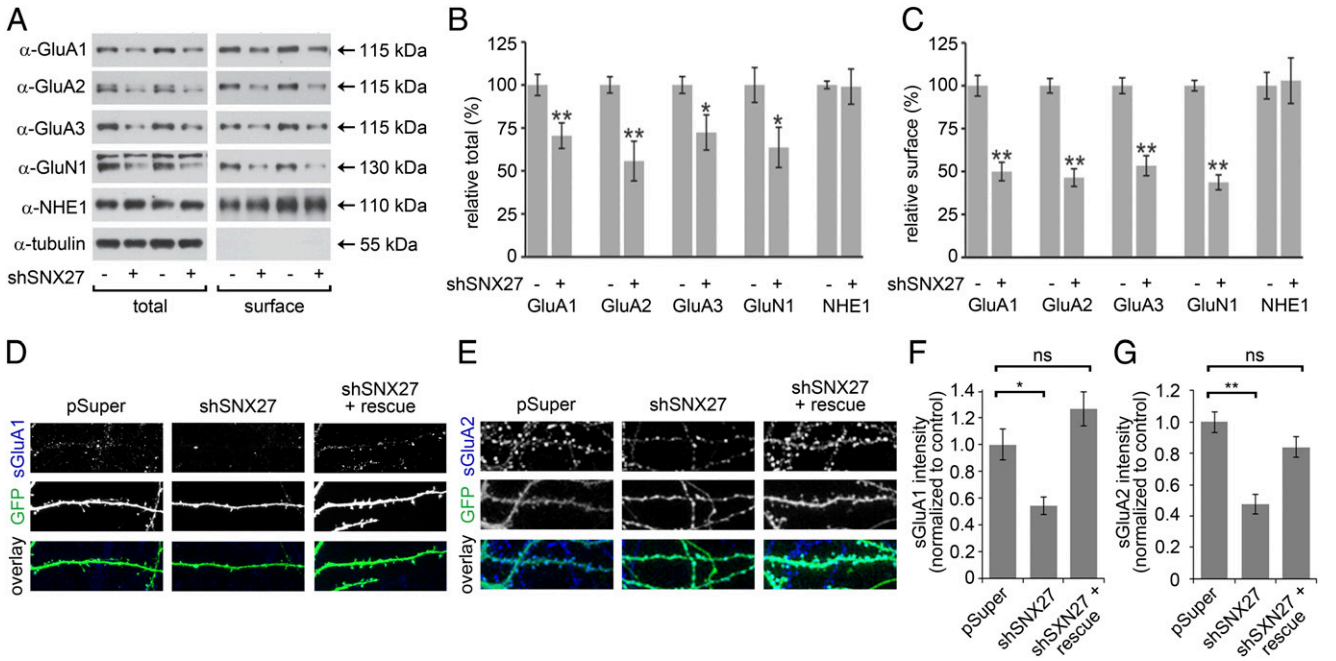

Fig. 4. Loss of SNX27 reduces glutamatergic receptor expression in neurons. (*A*) Rat cortical neurons transfected by electroporation with either vector control (pSuper) or shRNA directed against rat SNX27 (shSNX27) at DIV0 were grown until DIV14, and then treated by surface biotinylation. Total and surface proteins were visualized by Western blot. (*B* and *C*) Quantification of total (*B*) and surface protein levels (*C*). Error bars indicate ± SEM $*P < 0.05$, $**P < 0.005$ relative to pSuper control, ANOVA. $n = 4$. (*D* and *E*) Representative images of hippocampal neurons cotransfected with pSuper or shSNX27, with and without SNX27 rescue construct as indicated at top, along with GFP to visualize transfected cells. Surface immunostaining was performed with antibodies against endogenously expressed GluA1 (*D*) or GluA2 (*E*). Representative images are 40 μm dendritic segments. (*F* and *G*) Quantification of mean integrated sGluR1 (*F*) and sGluR2 (*G*) cluster intensity in dendritic segments normalized to pSuper. Error bars indicate ± SEM $*P < 0.05$, $**P < 0.005$ relative to pSuper control, ANOVA. $n \geq 12$ neurons for each.

withdrawal of glycine, the same time point when GluA1 and SNX27 interaction was clearly increased (Fig. 5 *B–D*). However, in neurons electroporated with SNX27 shRNA, sGluA1 levels were significantly reduced compared with control. Moreover, depletion of SNX27 completely blocked the cLTP-induced increase in sGluA1 (Fig. 5 *C* and *D*). Surface expression of mGluR5 was not effected by loss of SNX27 expression, demonstrating the specificity of SNX27 regulation toward GluA1 (Fig. 5*E*). Together, these results suggest that activity-dependent SNX27 binding is necessary for AMPA receptor delivery to the cell surface.

Discussion

The endosomal sorting network processes internalized plasma membrane proteins into endosomal bodies either for degradation or for recycling back to surface the plasma membrane (6, 7). Although the precise mechanisms governing AMPAR trafficking to synapses remain elusive, the C-terminal PDZ-ligand of AMPAR subunits is critical to their surface targeting and function (32, 33). An endosomal sorting protein dedicated to directing proteins along a PDZ-dependent recycling pathway would be expected to possess two fundamental properties (1): binding of the relevant receptor PDZ ligand and (2) influencing endosomal recycling and resulting receptor surface expression. We demonstrate that SNX27 binds AMPARs and facilitates surface trafficking through a mechanism requiring the PDZ- as well as PX-domain of SNX27. Notably, this function of SNX27 is distinct from established roles of other SNX family members. SNXs affect multiple aspects of endocytic membrane organization and regulation. For instance, several SNXs possess Bin/Amphiphysin/Rvs (BAR) domains that detect or induce membrane curvature (13). Although lacking a BAR domain, SNX27 is the only known family member to contain a PDZ domain (11, 37). To date, SNX27 modulates the early endosomal trafficking of Kir3 channels (22), 5-HT4a (15), and NR2C receptors (14), and consistent with our results was recently shown to increase delivery rate of AMPA receptors as well as β-adrenergic from endosomes to plasma membrane (16, 21, 38, 39). In each case, SNX27 acts as a PDZ-directed adaptor, binding the relevant PDZ motif on the receptor and guiding it through the endosomal pathway.

Here, we found that SNX27 is present in the cytosolic, membrane and PSD fractions of neurons. We demonstrate that increasing SNX27 expression enhanced surface expression of AMPARs. Conversely, depletion of endogenous SNX27 significantly reduced surface as well as total levels of AMPA and GluN1 receptors. This SNX27-mediated protein regulation was specific, as knockdown of SNX27 had no effect on the plasma membrane enriched protein NHE1 (27). Collectively, our data support a mechanism whereby cytosolic SNX27 is recruited to glutamatergic receptor containing endosomes to subsequently navigate these receptors to the synapse. Indeed, a recent study involving deletion of SNX27 in mice found reduced synaptic levels of AMPA and NMDA receptors (38). Additionally, SNX27 may critically maintain neuronal receptor levels by stabilizing their expression in recycling endosomes, at the cell surface, or by limiting their entry into the lysosome/proteasomal pathway, as has been suggested for other SNX27-mediated protein interactions (14, 16, 21, 23).

Our data demonstrate that SNX27 acts as an AMPAR recycling adaptor. For excitatory glutamatergic synapses, movement of AMPARs by way of recycling is essential for LTP (8). Given that LTP regulates synaptic AMPAR trafficking, we investigated whether neuronal activity similarly modulates SNX27-AMPARs binding and function. Chemical-induced LTP increased binding affinity of SNX27 for AMPAR, whereas loss of SNX27 completely abrogated cLTP-mediated AMPAR surface recruitment. Collectively, these findings suggest a role for SNX27 in general, as well as activity-mediated delivery of AMPARs to the plasma

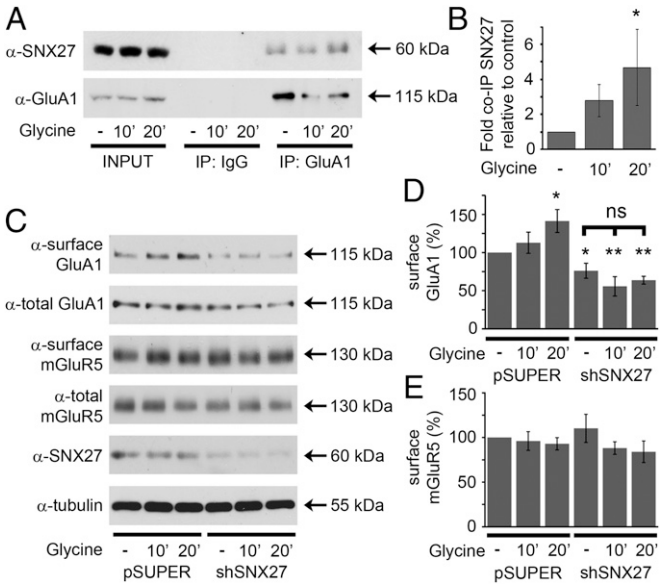

Fig. 5. Activity-dependent enhancement of surface AMPA requires SNX27 expression. (*A*) Representative immunoblots of SNX27 and GluA1 immunoprecipitation with GluA1 antibody from cortical neurons either unstimulated, or following 10 min or 20 min recovery after 5 min glycine-induced cLTP. Molecular weight of proteins indicated in kilodaltons (kDa) at right. (*B*) Quantification of fold SNX27 co-IP efficiency with GluA1. Error bars indicate ± SEM $*P < 0.05$, relative to unstimulated co-IP condition, ANOVA. $n = 7$. (*C*) Rat cortical neurons electroporated with control pSuper vector or shSNX27 were treated at DIV14 with glycine for 5 min to induce cLTP and recovered 10 or 20 min before cell-surface biotinylation. Total and surface proteins were visualized by Western blot. (*D* and *E*) Quantification of GluA1 (*D*) and mGluR5 (*E*) surface levels. Error bars indicate ± SEM $*P < 0.05$, $**P < 0.005$ relative to pSuper control, ANOVA. $n = 4$.

membrane, perhaps to enable induction of early burst and long-term maintenance of synaptic potentiation. These findings shed light on a SNX mediated-mechanism by which AMPARs are guided to the plasma membrane, allowing for activity-dependent changes to occur. Notably, LTP plays a prominent role in pathological learning and memory, including addiction and posttraumatic stress disorders. Identifying molecular components regulating trafficking, particularly those recruited during LTP, may reveal novel therapeutic targets as well as provide insight into these disorders.

Materials and Methods

Antibodies. Commercial antibodies HA.11 (Covance), c-myc (Santa Cruz), mGluR5 (Abcam), NHE1 (BD Biosciences), SNX27a (Novus Bio and GeneTex), and tubulin (Sigma-Aldrich) were used. Specific monoclonal against N-terminal GluA1 (4.9D) and GluA2 (6A), and polyclonal antibodies against GFP (JH4030), GluA1 (JH4294 and 4.9D), GluA3 (JH4300), and GluN1 (JH4456) were generated in-house after antisera purchase from Covance.

Plasmids. Full-length SNX27a and SNX27b were cloned from a randomly primed Sprague–Dawley rat hippocampal cDNA library and SNX72a was inserted into modified myc-pRK5 and pEGFP-C1 (Clontech). Human SNX27a, SNX27aΔPX deletion (Δ163–272) and SNX27a encoding a point mutation in the PDZ ligand (H112A) were a gift from Mark Von Zastrow (University of California at San Francisco School of Medicine, San Francisco). Human Snx27a was subcloned into GFP-pRK5 vector, ΔPX deletion and PDZ point-mutation were introduced by ligation into human GFP-SNX27 through SacII-PpuMI restriction digest. Oligonucleotides were annealed and cloned into HindIII and BglII sites of pSuper to make SNX27 shRNA: sense 5′-GATCTAACCAGGTAATAGCGTTTGAACTCGAGTTCAAACGCTATTACCTGGTTTTTTTC-3′ and antisense 5′-TCGAGAAAAAAACCAGGTAATAGCGTTTGAACTCGAGTTCAAACGCTATTACCTGGTTA-3′. shRNA-resistant rat myc-tagged SNX27 was generated by Quickchange site directed mutagenesis with primers: 5′-GGGCAGCTGGAGAACCAAGTGATCGCATTCGAATGGGATGAGATGC-3′ and 5′-GCATCTCATCCCATTCGAATGCGATCACTTGGTTCTCCAGCTGCCC-3′.

GST Pull-Down Assays from Rat Brain Lysate. Bacterial GST fusion proteins encoding the last 50 amino acids of GluR2 C terminus was constructed and purified as described (40). Total adult rat brain extract was prepared by glass Teflon homogenizing brain tissue in 10 volumes of ice-cold pull-down buffer [1% (vol/vol) Triton X-100, 1 mM EDTA, 1 mM EGTA, 50 mM NaF, and 5 mM Na-pyrophosphate in PBS] supplemented with 1 μg/mL leupeptin, 0.1 μg/mL aprotinin, 1 μg/mL phenylmethanesulfonyl fluoride, and 1 μg/mL pepstatin. Homogenate was centrifuged twice at 75,600 × *g* for 30 min at 4 °C and resulting supernatant incubated with immobilized recombinant GST or GST-GluA2 proteins overnight at 4 °C, followed by ice-cold pull-down buffer washes before 2× SDS sample buffer elution. Bound proteins were resolved by 7.5–15% gradient SDS/PAGE stained with colloidal Coomassie blue. Identification of GST-GluA2 interacting proteins was done by in-gel trypin digestion of gel bands and liquid chromatography/tandem mass-spectrometry (LC/MS-MS) before database searching at the Taplin Mass Spectrometry Facility (Harvard University).

Rat Brain Fractionation and Immunoprecipitation of Endogenous Protein. Rat brain was homogenized in 10 w/vol ice-cold Nonidet P-40/DOC buffer (1× PBS, 1 mM EDTA, 1 mM EGTA, 1 mM sodium vanadate, 5 mM sodium pyrophosphate, 50 mM NaF, 1% Nonidet P-40, 0.5% deoxycholic acid supplemented with 1 μg/mL leupeptin, 0.1 μg/mL aprotinin, 1 μg/mL phenylmethanesulfonyl fluoride, and 1 μg/mL pepstatin) by glass homogenizer. Centrifugation at 17,000 × *g* for 10 min cleared homogenate and soluble fractions were collected for immunoprecipitation. Endogenous proteins were immunoprecipitated overnight at 4 °C using 2 μL of antibody per reaction and washed with Nonidet P-40/DOC buffer and resuspended in 2× SDS loading buffer.

Cell Culture, Electroporation, and Transient Transfection. HEK 293T cells were grown in DMEM supplemented with 10% (vol/vol) FBS, 2 mM Glutamax, 50 U/mL penicillin, and 50 μg/mL streptomycin. Cells were transfected using Lipofectamine 2000 (Invitrogen) according to the manufacturer's instructions, and processed 48 h later.

E18 rat pup cortical neurons were plated on poly-L-lysine coated dishes in NM5 media [Neurobasal growth medium (Invitrogen) supplemented with 2% B27 (Invitrogen), 2 mM Glutamax (GIBCO), 50 U/mL PenStrep (GIBCO), and 5% Fetal Horse Serum (HyClone)]. At day in vitro (DIV) 3–4, neurons were treated with 5 μM uridine and 5 μM (+)-5-fluor-2′-deoxyuridine in NM1 (Neurobasal supplemented with 2% B27, 2 mM Glutamax, 50 U/mL PenStrep, and 1% Horse Serum) for 3 d. Every 3–4 DIV thereafter, half of the culture media was changed with glia conditioned NM1 until DIV 18–20. Dissociated cortical culture was electroporated at DIV 0 using Rat Neuron Nucleofector kit according to manufacturer's protocol (Lonza Group).

Dissociated E19 rat pup hippocampal neurons plated onto poly-L-lysine coated glass coverslips were cultured in Neurobasal Medium with B27, 0.5 mM glutamine, and 12.5 μM glutamate. Neurons were Lipofectamine 2000 (Invitrogen) transfected at DIV 18–19 according to the manufacturer's instructions, and processed 48 h later.

Cultured cells harvested 24 h posttransfection (HEK cells) or at DIV 18–20 (cortical neurons) were processed similarly to brain fractionation experiments. Briefly, cells were extracted in Nonidet P-40/DOC buffer and rocked at 4 °C for 30 min before 15 min centrifugation at 16,000 × g. Supernatants were incubated with antibodies, protein A- or G-Sepharose overnight at 4 °C, washed with ice-cold Nonidet P-40/DOC buffer and eluted in 2× SDS sample buffer. Immunoprecipitated proteins were resolved by SDS/PAGE and Western blot analysis.

Chemical LTP Stimulation. Cultured cortical neurons were incubated 20 min in ACSF (125 mM NaCl, 2.5mM KCl, 1.5 mM CaCl2, 25 mM Hepes, pH 7.4, 33 mM Glucose, 1 mM MgCl, 500 nM TTX, 20 μM Bicuculine, 1 μM Strychnine) before 5-min chemical LTP induction in magnesium-free ACSF supplemented with 200uM glycine (cLTP-ACSF). Neurons recovered in ASCF 10 or 20 min before lysis in NL buffer (1× PBS, 1 mM EDTA, 1 mM EGTA, 1 mM Sodium vanadate, 5 mM Sodium pyrophosphate, 50 mM NaF, 1% Triton X-100 supplemented with 1 μg/mL leupeptin, 0.1 μg/mL aprotinin, 1 μg/mL phenylmethanesulfonyl fluoride, and 1 μg/mL pepstatin).

Immunostaining, Microscopy, and Quantification. Hippocampal neurons fixed in 4% paraformaldehyde/4% sucrose were incubated with primary antibodies overnight at 4 °C in 1× GDB buffer [15 mM phosphate buffer (pH 7.4) containing 0.1% gelatin, 0.3% Triton X-100, and 0.25 M NaCl], followed by secondary antibodies for 2–4 h. For surface staining of endogenous

AMPAR, neurons were fixed for 5 min and incubated with either N-terminal-GluA1 or GluA2-antibody overnight in 1× GDB buffer lacking Triton X-100. All subsequent primary and secondary antibody incubations were in 1× GDB buffer as described.

Confocal z-series image stacks of neurons taken with an LSM510 confocal microscope system (Zeiss) were compressed and analyzed using MetaMorph software (Universal Imaging). For surface integrated intensity quantification (i.e., average cluster intensity per unit area), different immunostained channels were parsed into separate images. Five dendritic segments of 50 μm collected from at least 20 neurons per condition were outlined and thresholded for each channel within an experiment to exclude diffuse background staining. Statistical significance was calculated using ANOVA.

PSD Fractionation. Cultured rat cortical neurons harvested in buffer [320 mM sucrose, 10 mM Hepes pH 7.4, 5 mM sodium pyrophosphate, 1 mM EDTA, protease inhibitor mixture (Roche), 200 nM okadaic acid], were homogenized using a 26.5-gauge needle. Homogenate was centrifuged at 800 × *g* for 10 min yielding P1 and S1. S1 was centrifuged at 17,000 × *g* for 20 min to yield P2 and S2. P2 was resuspended in water was quickly adjusted to 4 mM Hepes pH 7.4, followed by 30-min agitation. Lysed P2 fraction collected by centrifugation at 25,000 × *g* for 20 min. The resulting pellet was resuspended in 50 mM Hepes pH 7.4 and an equal volume of 1% triton X-100, and agitated for 10 min. PSD fractions were obtained by centrifugation at 32,000 × *g* for 20 min.

Biotinylation Assays. Cortical cultures washed once with fresh PBSCM (1× PBS, 1mM $MgCl_2$, 0.1mM $CaCl_2$, pH 8.0) were incubated with cleavable NHS-SS-biotin (0.5 mL/mL, Thermo Scientific) 30 min at 4 °C. Neurons then incubated with PBSCM and 20 mM glycine to quench the reaction, and quickly washed with PBSCM. Neurons were lysed (1× PBS, 1 mM EDTA, 1 mM EGTA, 1 mM Sodium vanadate, 5 mM Sodium pyrophosphate, 50 mM NaF, 1% Nonidet P-40, 0.5% DOC) and cleared by 10-min centrifugation at 17,000 × *g*, 4 °C. Equal amounts of protein incubated 4 °C with neutravidin agarose beads (Thermo Scientific) overnight and washed with lysis buffer, and biotinylated surface proteins were eluted in 2× SDS loading buffer. Lysates not subjected to neutravidin beads were analyzed as a measure of total cellular protein levels.

Western blot films were scanned and digital signal intensities measured using Image J (National Institutes of Health). The intensities of experimental conditions were divided by the intensities of input conditions/controls from the Western blot regions to find the normalized intensities for surface GluA1, GluA2, GluA3, Nhe1, etc. and for relative co-IP binding assessment. All statistics were performed using excel. Paired *t* tests were used to assess the significance of quantified Western blots. Critical value, α, was set at 0.05 for all significance testing.

ACKNOWLEDGMENTS. This work was supported by grants from the National Institutes of Health, the Howard Hughes Medical Institute (to R.L.H.), and the John T. Reid Charitable Trusts (to V.A.). V.A. was supported by fellowships from the International Human Frontier Science Program (LT00399/2008-L) and the Australian National Health and Medical Research Council (ID. 477108). G.H.D. is supported by a postdoctoral fellowship from the Canadian Institute for Health Research.

1. Anggono V, Huganir RL (2012) Regulation of AMPA receptor trafficking and synaptic plasticity. *Curr Opin Neurobiol* 22(3):461–469.
2. Lledo PM, Zhang X, Südhof TC, Malenka RC, Nicoll RA (1998) Postsynaptic membrane fusion and long-term potentiation. *Science* 279(5349):399–403.
3. Lee HK, et al. (2003) Phosphorylation of the AMPA receptor GluR1 subunit is required for synaptic plasticity and retention of spatial memory. *Cell* 112(5):631–643.
4. Lüscher C, et al. (1999) Role of AMPA receptor cycling in synaptic transmission and plasticity. *Neuron* 24(3):649–658.
5. Kessels HW, Malinow R (2009) Synaptic AMPA receptor plasticity and behavior. *Neuron* 61(3):340–350.
6. Hanley JG (2010) Endosomal sorting of AMPA receptors in hippocampal neurons. *Biochem Soc Trans* 38(2):460–465.
7. van der Sluijs P, Hoogenraad CC (2011) New insights in endosomal dynamics and AMPA receptor trafficking. *Semin Cell Dev Biol* 22(5):499–505.
8. Park M, Penick EC, Edwards JG, Kauer JA, Ehlers MD (2004) Recycling endosomes supply AMPA receptors for LTP. *Science* 305(5692):1972–1975.
9. Wang Z, et al. (2008) Myosin Vb mobilizes recycling endosomes and AMPA receptors for postsynaptic plasticity. *Cell* 135(3):535–548.
10. Correia SS, et al. (2008) Motor protein-dependent transport of AMPA receptors into spines during long-term potentiation. *Nat Neurosci* 11(4):457–466.
11. Teasdale RD, Collins BM (2012) Insights into the PX (phox-homology) domain and SNX (sorting nexin) protein families: Structures, functions and roles in disease. *Biochem J* 441(1):39–59.
12. Ponting CP (1996) Novel domains in NADPH oxidase subunits, sorting nexins, and PtdIns 3-kinases: Binding partners of SH3 domains? *Protein Sci* 5(11):2353–2357.
13. van Weering JR, Verkade P, Cullen PJ (2010) SNX-BAR proteins in phosphoinositide-mediated, tubular-based endosomal sorting. *Semin Cell Dev Biol* 21(4):371–380.
14. Cai L, Loo LS, Atlashkin V, Hanson BJ, Hong W (2011) Deficiency of sorting nexin 27 (SNX27) leads to growth retardation and elevated levels of N-methyl-D-aspartate receptor 2C (NR2C). *Mol Cell Biol* 31(8):1734–1747.
15. Joubert L, et al. (2004) New sorting nexin (SNX27) and NHERF specifically interact with the 5-HT4a receptor splice variant: Roles in receptor targeting. *J Cell Sci* 117(Pt 22): 5367–5379.
16. Lauffer BE, et al. (2010) SNX27 mediates PDZ-directed sorting from endosomes to the plasma membrane. *J Cell Biol* 190(4):565–574.
17. Lunn ML, et al. (2007) A unique sorting nexin regulates trafficking of potassium channels via a PDZ domain interaction. *Nat Neurosci* 10(10):1249–1259.
18. Valdes JL, et al. (2011) Sorting nexin 27 protein regulates trafficking of a p21-activated kinase (PAK) interacting exchange factor (β-Pix)-G protein-coupled receptor kinase interacting protein (GIT) complex via a PDZ domain interaction. *J Biol Chem* 286(45):39403–39416.
19. Sheng M, Sala C (2001) PDZ domains and the organization of supramolecular complexes. *Annu Rev Neurosci* 24:1–29.
20. Ye F, Zhang M (2013) Structures and target recognition modes of PDZ domains: Recurring themes and emerging pictures. *Biochem J* 455(1):1–14.
21. Nakagawa T, Asahi M (2013) β1-adrenergic receptor recycles via a membranous organelle, recycling endosome, by binding with sorting nexin27. *J Membr Biol* 246(7): 571–579.
22. Nassirpour R, Slesinger PA (2007) Subunit-specific regulation of Kir3 channels by sorting nexin 27. *Channels (Austin)* 1(5):331–333.
23. Steinberg F, et al. (2013) A global analysis of SNX27-retromer assembly and cargo specificity reveals a function in glucose and metal ion transport. *Nat Cell Biol* 15(5): 461–471.
24. Rincón E, et al. (2007) Proteomics identification of sorting nexin 27 as a diacylglycerol kinase zeta-associated protein: New diacylglycerol kinase roles in endocytic recycling. *Mol Cell Proteomics* 6(6):1073–1087.
25. MacNeil AJ, Mansour M, Pohajdak B (2007) Sorting nexin 27 interacts with the Cytohesin associated scaffolding protein (CASP) in lymphocytes. *Biochem Biophys Res Commun* 359(4):848–853.
26. Zimmerman SP, Hueschen CL, Malide D, Milgram SL, Playford MP (2013) Sorting nexin 27 (SNX27) associates with zona occludens2 (ZO2) and modulates the epithelial tight junction. *Biochemical journal*.
27. Brett CL, Donowitz M, Rao R (2005) Evolutionary origins of eukaryotic sodium/proton exchangers. *Am J Physiol Cell Physiol* 288(2):C223–C239.
28. Oh MC, Derkach VA, Guire ES, Soderling TR (2006) Extrasynaptic membrane trafficking regulated by GluR1 serine 845 phosphorylation primes AMPA receptors for long-term potentiation. *J Biol Chem* 281(2):752–758.
29. Man HY, et al. (2003) Activation of PI3-kinase is required for AMPA receptor insertion during LTP of mEPSCs in cultured hippocampal neurons. *Neuron* 38(4):611–624.
30. Lin H, Huganir R, Liao D (2004) Temporal dynamics of NMDA receptor-induced changes in spine morphology and AMPA receptor recruitment to spines. *Biochem Biophys Res Commun* 316(2):501–511.
31. Shi SH, et al. (1999) Rapid spine delivery and redistribution of AMPA receptors after synaptic NMDA receptor activation. *Science* 284(5421):1811–1816.
32. Shi S, Hayashi Y, Esteban JA, Malinow R (2001) Subunit-specific rules governing AMPA receptor trafficking to synapses in hippocampal pyramidal neurons. *Cell* 105(3): 331–343.
33. Hayashi Y, et al. (2000) Driving AMPA receptors into synapses by LTP and CaMKII: Requirement for GluR1 and PDZ domain interaction. *Science* 287(5461):2262–2267.
34. Huganir RL, Nicoll RA (2013) AMPARs and synaptic plasticity: The last 25 years. *Neuron* 80(3):704–717.
35. Lu W, et al. (2001) Activation of synaptic NMDA receptors induces membrane insertion of new AMPA receptors and LTP in cultured hippocampal neurons. *Neuron* 29(1):243–254.
36. Liao D, Scannevin RH, Huganir R (2001) Activation of silent synapses by rapid activity-dependent synaptic recruitment of AMPA receptors. *J Neurosci* 21(16):6008–6017.
37. Cullen PJ, Korswagen HC (2012) Sorting nexins provide diversity for retromer-dependent trafficking events. *Nat Cell Biol* 14(1):29–37.
38. Wang X, et al. (2013) Loss of sorting nexin 27 contributes to excitatory synaptic dysfunction by modulating glutamate receptor recycling in Down's syndrome. *Nat Med* 19(4):473–480.
39. Loo LS, Tang N, Al-Haddawi M, Dawe GS, Hong W (2014) A role for sorting nexin 27 in AMPA receptor trafficking. *Nat Commun* 5:3176.
40. Anggono V, et al. (2006) Syndapin I is the phosphorylation-regulated dynamin I partner in synaptic vesicle endocytosis. *Nat Neurosci* 9(6):752–760.